Appl Compos Mater (2011) 18:113–125
DOI 10.1007/s10443-010-9135-1

A Global/Local Finite Element Approach for Predicting Interlaminar and Intralaminar Damage Evolution in Composite Stiffened Panels Under Compressive Load

Elisa Pietropaoli · Aniello Riccio

Received: 23 December 2009 / Accepted: 17 March 2010 / Published online: 15 April 2010
© Springer Science+Business Media B.V. 2010

Abstract This paper addresses the prediction of intralaminar and interlaminar damage onset and evolution in composite structures through the use of a finite element based procedure. This procedure joins methodologies whose credibility has been already assessed in literature such as the Virtual Crack Closure Technique (for delamination) and the ply discount approach (for matrix/fiber failures). In order to establish the reliability of the procedure developed, comparisons with literature experimental results on a stiffened panel with an embedded delamination are illustrated. The methodology proposed, implemented in ANSYS © as post-processing routines, is combined with a finite element model of the panel, built by adopting both shell and solid elements within the frame of an embedded global/local approach to connect differently modelled substructures.

Keywords Layered structures · Delamination · Buckling · Damage mechanics · Finite element analysis

1 Introduction

The damage phenomenology of composite material structures is very complex because it entails a multimode fracture process characterized by the presence of both intralaminar and interlaminar damage which can onset, propagate and interact each other.

It is well known that as consequence of low velocity impact, composites always display a damage pattern characterised by the presence of both matrix failures and delaminations [1]. Therefore it could be argued that an accurate prediction of the residual stiffness and strength of delaminated structures under compressive loads could require that both intralaminar and interlaminar damage be taken into account as well as effect of their possible interaction.

E. Pietropaoli (✉) · A. Riccio
CIRA Italian Aerospace Research Center, via Maiorise, 81043 Capua, Italy
e-mail: e.pietropaoli@cira.it

A. Riccio
e-mail: a.riccio@cira.it

A great amount of literature works have been devoted to the analysis of the post-buckling behaviour of structures with embedded delamination [2–8] but only in a few cases the presence of intralaminar damage has been considered too [9–12].

Finite element procedures dealing with the delamination growth are generally based on fracture mechanics concepts and involve the evaluation of the Strain Energy Release Rates (ERR) at the delamination front [13]. Some approaches do not take into account the modes separation and evaluate only a total value of the ERR [10] while other techniques such as the Virtual Crack Closure Technique (VCCT) [14] allow the ERRs to be computed distinguish between the three basic fracture modes (GI,GII and GIII). The growth initiation is identified on the basis of a growth criterion [15] (which can be considered as a curve fit to fracture tests data): when a prescribed function of the computed ERRs overcomes a threshold value dependent on the fracture toughness of the material (GIC,GIIC and GIIIC), the delamination front is modified thus simulating the delamination opening.

The modification of delamination front can be obtained by a moving mesh method as proposed in Ref. [9, 10] or by releasing not merged nodes laying in the same position (i.e. having the same coordinates) but belonging to two different fracture surfaces [5, 11, 12, 16].

When dealing with delaminated structures, overlaps can be induced between the debonded layers, therefore contact elements must be used in the finite element model to obtain meaningful results [3, 4]. The introduction of these elements enhances the agreement of the numerical results with respect to the experimental ones but induces numerical convergence problems thus requiring a very stable nonlinear solver.

Concerning the intralaminar damage, different failure criteria are available in literature for the individuation of the first ply failure load such as the Hashin's criteria [17, 18] whose peculiar characteristic is that they allow distinguishing among different failure modes.

It is well known that composite plates retain residual stiffness and strength after the occurrence of the first ply failure. A widely used approach, for the simulation of the behaviour of composite structures beyond the detection of the first ply failure, consists in the change of the material properties for failed elements according to suitable degradation rules (ply discount approach) [19]. This approach has been extensively used for the analysis of composite plates with holes [19–27] but only in a few cases it has been applied to the analysis of delaminated plates [10, 12].

The numerical simulation of the compression after impact behaviour of composite plates requires that all these features (evaluation of the ERRs, failure check and degradation approach) be included into an iterative non linear procedure.

The stiffness and strength reduction associated to the presence of a delamination in composite laminate plates is very strong especially in compression. In order to generate experimental data to be used for validating numerical models dealing with delamination, experimental tests are generally performed by creating an artificial debonding between two adjacent layers of a composite laminate through the insertion of a very thin film of Teflon [2, 28]. The composite laminate is thus subdivided into a thin sub-laminate and a thick sublaminate or base sublaminate. Two edges of the structure are then clamped in a test machine and a compressive displacement is gradually applied. The behaviour commonly observed during these tests can be described as follows. As the load increases the thin sublaminate buckles first. Afterwards, the buckling of the base sublaminate is induced. In this case, depending on the thicknesses ratio of the two sub-laminates, the out of plane displacement of the base sublaminate can be of the same sign (Type I) or of different sign (Type II) with respect to the one of the thin sub-laminate. When the buckling is of Type II,

an increase in applied load determines the condition known as global buckling: the thin sublaminate is dragged towards the base sublaminate but the delamination opening continues to be relevant.

The delamination starts growing generally after the global buckling but propagation after the local buckling could be also possible for different constraints or delamination shapes depending on the stress distribution at the delamination front. In the same way, intralaminar damages, depending on the stress state within the material can be induced before or after the delamination growth.

Within this work a numerical procedure is adopted [12], based on the combined use of the Virtual Crack Closure Technique and of a ply discount approach. The occurrence of matrix cracks, fibre breakages and all the others intralaminar failures are verified (see Table 1) for each ply of the laminate at each load step of a non linear incremental analysis. Furthermore, the material properties of the damaged ply are reduced according to suitable degradation rules depending on the failure mode detected in order to simulate the progressive decrease of the structural stiffness associated to the presence of damaged areas [4, 5]. On the other hand, by considering the interlaminar damage as a fracture process, fracture mechanics concepts are used [14] and the Strain Energy Release Rate is monitored (Table 1) to define the delamination growth status (firstly its initiation and after how it grows). After the growth initiation the delamination shape is modified by using a fail-release approach which merely consists in releasing connections (usually multipoint constraints) which kept together nodes with identical coordinates but not merged on the delamination interface.

The procedure above deployed has been implemented in ANSYS as user subroutines, with the aim to investigate the intralaminar and interlaminar damage evolution in a geometrically complex structure such as a stiffened composite panel characterized by the presence of an embedded delamination subjected to static compressive loads. Literature experimental data were available for this structure both in terms of buckling loads and damage characterisation [28].

In order to mitigate the computational efforts requested by numerical analyses, a global/local strategy [29] has been adopted to build the finite element model.

Usually global/local is accounted as synonymous of sub-structuring [16]: mainly a detailed local model receives as boundary conditions the deformation field obtained by a global model of the full structure thus defining a sequential global/local procedure which does not allow effects of the local model on the global one to be taken into account. An embedded global/local procedure is surely more suitable but requires the availability of interface elements or rather coupling elements able to take into account also large

Table 1 Failure criteria and degradation rules

Failure Mode	Criterion		Degradation rule
Matrix tensile and compressive failure	$\left(\frac{\sigma_{yy}}{Y_t}\right)^2+\left(\frac{\sigma_{xy}}{S_{xy}}\right)^2+\left(\frac{\sigma_{yz}}{S_{yz}}\right)^2\geq 1$	$\left(\frac{\sigma_{yy}}{Y_c}\right)^2+\left(\frac{\sigma_{xy}}{S_{xy}}\right)^2+\left(\frac{\sigma_{yz}}{S_{yz}}\right)^2\geq 1$	$\overline{E}_y = kE_y; \overline{E}_z = kE_z$
Fibre tensile and compressive failure	$\left(\frac{\sigma_{xx}}{X_t}\right)^2+\left(\frac{\sigma_{xy}}{S_{xy}}\right)^2+\left(\frac{\sigma_{xz}}{S_{xz}}\right)^2\geq 1$	$\left(\frac{\sigma_{xx}}{X_c}\right)^2\geq 1$	$\overline{G}_{yz} = kG_{yz}$ $\overline{E}_x = kE_x$ $\overline{G}_{xy} = kG_{xy}; \overline{G}_{xz} = kG_{yz}$
Fibre-matrix shear-out failure	$\left(\frac{\sigma_{xx}}{X_c}\right)^2+\left(\frac{\sigma_{xy}}{S_{xy}}\right)^2+\left(\frac{\sigma_{xz}}{S_{xz}}\right)^2\geq 1$		$\overline{G}_{xy} = G_{yz}$ $\overline{G}_{xz} = G_{yz}$
Fibre Kinking failure	$\left(\frac{\sigma_{xx}}{X_c}\right)^2+\left(\frac{\sigma_{xz}}{S_{xz}}\right)^2\geq 1$		$\overline{E}_x = kE_x; \overline{E}_y = kE_y;$ $\overline{E}_z = kE_z; \overline{G}_{xy} = kG_{yz};$ $G_{xz} = kG_{yz}; \overline{G}_{yz} = kG_{yz}$
Delamination growth	$\left(\frac{G_I}{G_{IC}}\right)+\left(\frac{G_{II}}{G_{IIC}}\right)+\left(\frac{G_{III}}{G_{IIIC}}\right)=E_d\geq 1$		

deformations in non linear analyses and to connect different type of elements such as shell and solid.

This paper starts (Section 2) with the description of the finite element model of the stiffened panel built by adopting an embedded global/local technique, and ends presenting numerical results (Section 3) focusing on interlaminar and intralaminar failure modes and effects of their interaction. Comparisons against experimental results taken from Ref. [28] are also provided.

2 Problem Definition and Finite Element Model Description

The compressive behaviour of a stiffened panel, whose geometrical dimensions are indicated in Fig. 1, has been investigated taking into account the presence of an embedded defect (delamination) placed between the forth and the fifth ply (90°/45°) of the composite laminate of which the skin of the panel is made. This kind of benchmark has been selected due to the availability in literature of accurate experimental results [28] in terms of both mechanical response of the whole structure and damage characterization. Material properties for the HTA-6376C are reported in Table 2 together with strength and critical fracture toughnesses requested for the intralaminar/interlaminar damage analysis.

The schematization of the panel shown in Fig. 1 reflects the choice to use, in the finite element discretization, respectively hexahedral elements for the modelization of stringers and delamination and shell elements for the surrounding undamaged skin (see Fig. 2).

The presence of an embedded delamination which can grow and the need to obtain a correct prediction of the three dimensional stress state within the material, from which depends both the occurrence of intralaminar damages and the progression of the delamination front, has led to the adoption of hexahedral elements for the delaminated area. The initial delamination area of radius R_0 and the circular crown around it are modeled by maintaining couples of nodes with identical coordinates not merged on

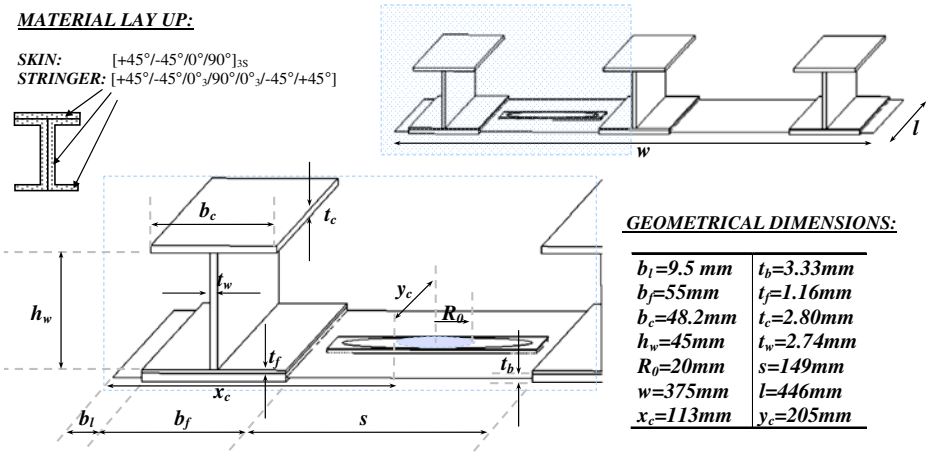

Fig. 1 Stiffened panel geometrical dimensions and material lay up defined respect to the applied load direction- SFN3 configuration [28]

Table 2 Material properties (HTA-6376C) [30, 31]

Longitudinal tensile modulus	140 GPa	Longitudinal tensile strength	2100 MPa
Transverse tensile modulus	10.5 GPa	Transverse tensile strength	70 MPa
Poisson ratio 12 and 13	0.3	Longitudinal compressive strength	1650 MPa
Poisson ratio 23	0.51	Transverse compressive strength	240 MPa
In plane shear modulus 12–13	5.2 GPa	In plane shear strength	105 MPa
In plane shear modulus 2–3	3.48 GPa	Critical ERR–Mode I	260 J/m^2
		Critical ERR–Mode II	950 J/m^2

adjacent faces of the two sub-laminates in which the skin of the panel is subdivided (Fig. 3).

Contact elements have been placed on the initial delamination area in order to avoid overlaps which could occur during the load application whereas interface elements (MPCs) have been used to keep together (Fig. 3-a) the two sub-laminates in the circular crown (radius Rmax-R_0) where the delamination is expected to grow and after to release them (Fig. 3-b) whether the delamination growth criterion is satisfied (fail release approach).

Really, three-dimensional elements have been adopted also for the stringers in order to obtain a model which in future research activities could be used to take into account both skin-stiffener debonding and intralaminar damage in these structural components.

Then, shell and hexahedral elements have been connected by using interface elements based on coupling equations between the degrees of freedoms (rotational and translational) of nodes at common boundaries [29].

Three analysis approaches have been adopted. The first approach (CH) does not allow the delamination to grow (CH): indeed, the delaminated area during the analysis remains unchanged (radius R_0 Fig. 3). In what follows two other approaches are introduced: DEL and PDADEL which both made use of the fail release approach to predict and simulate the delamination propagation. Only the latter approach takes into account also the onset and progression of intralaminar damage.

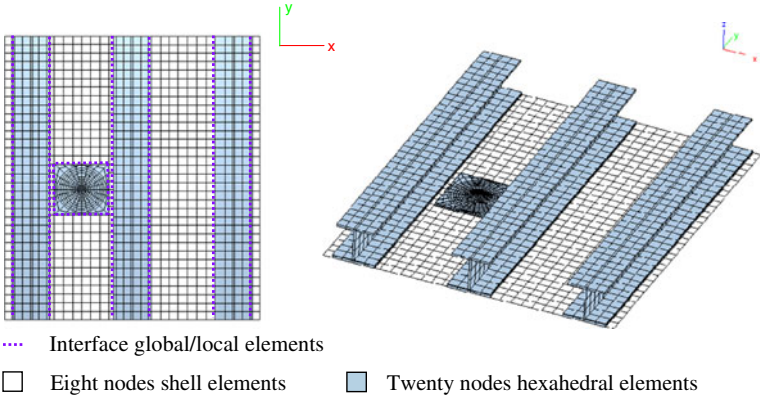

Fig. 2 Finite element discretization: solid and shell elements connected at common boundaries using interface elements

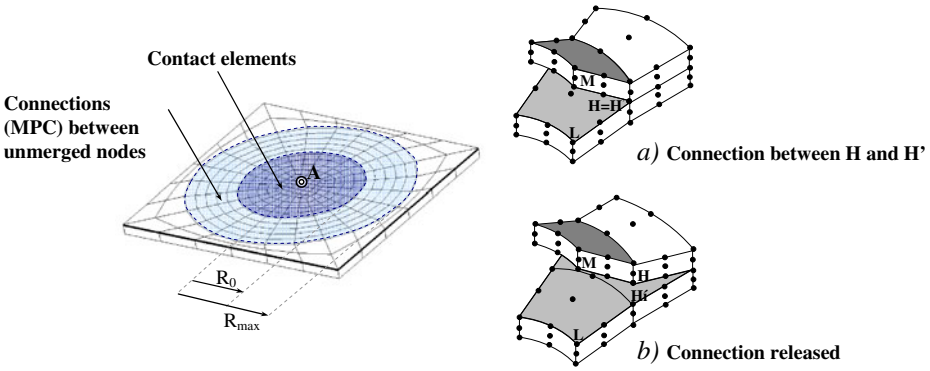

Fig. 3 Delamination modellization (the position of a control point A placed in the centre of the delaminated area is also sketched)

3 Numerical Results

3.1 Comparison Between Numerical and Experimental Results

The comparison between the applied-strain versus load graph experimental and numerical (CH approach) curve is shown in Fig. 4. The global buckling of the panel is reached at −2773 με which is very close to the experimental value −2850 με.

A good agreement has been found also in terms of local-buckling load (numerical: −1178 με experimental: −1250 με) as clearly visible in the Fig. 5 where the out of plane displacement of the control point A (see Fig. 3) is plotted against the applied compressive strain.

The deformed shapes experienced by the panel at the local buckling load and in the post buckling regime are presented in Fig. 6. At the local buckling load, the instability is detected only in the delaminated region where the thin sub-laminate starts to behave an out of plane displacement directed towards the inner side of the panel. This displacement

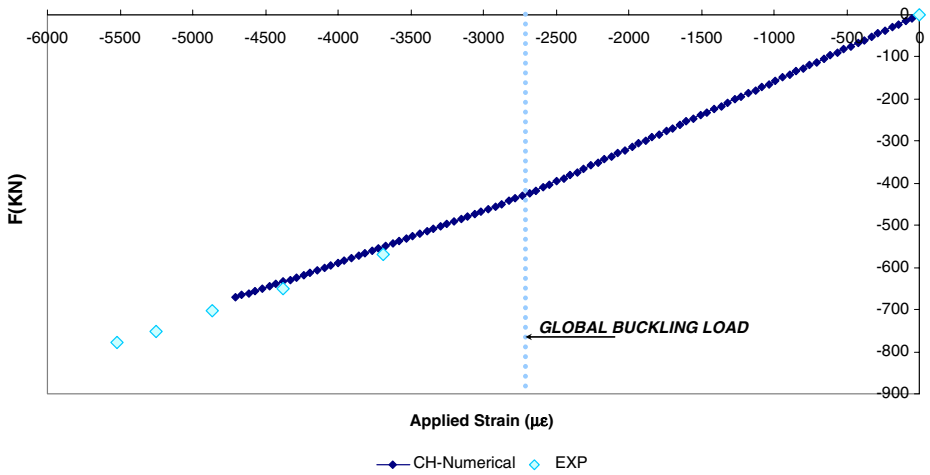

Fig. 4 Applied-strain/Load graph: comparison between numerical and experimental results

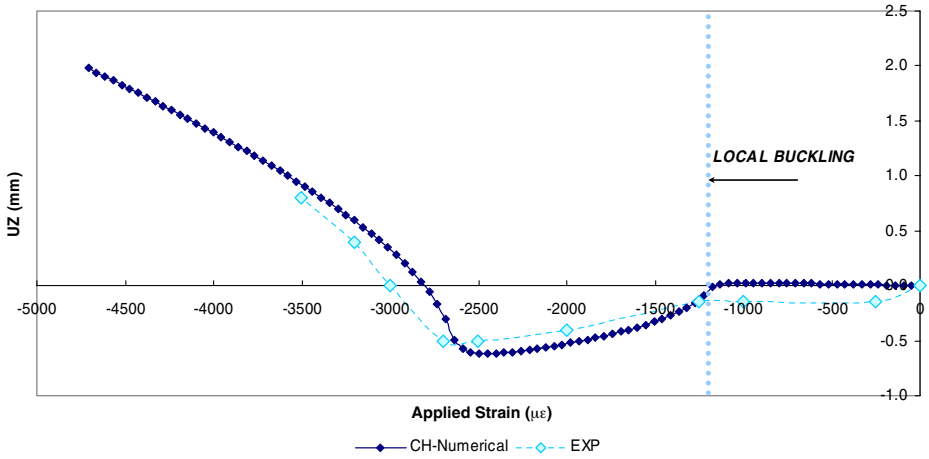

Fig. 5 Applied-strain/Out of plane displacement of the point A: comparison between numerical and experimental results

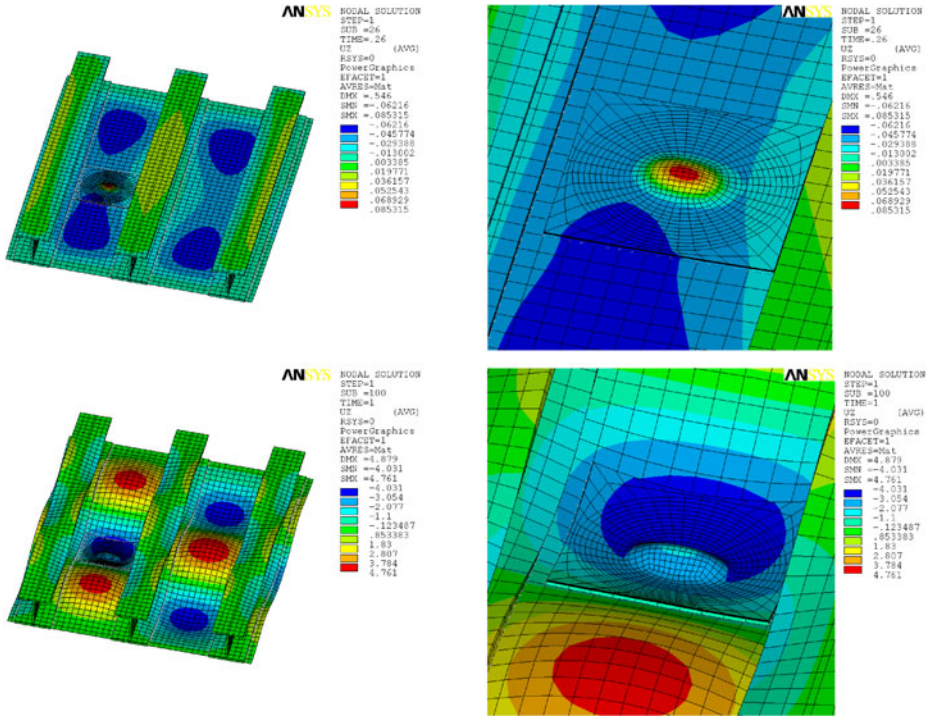

Fig. 6 Deformed shape with out of plane displacement contour at −1177 με (top) [local buckling of the delamination] and −4611.43 με [post-buckling for the panel] (bottom). The pictures on the right are enlargements of the delaminated area at the same applied strain

increases with the load, up to the reaching of the global-buckling condition when the whole panel goes to buckling too. By then, the thin sub-laminate is obliged to follow the buckle shape of the skin of the panel which causes an inversion in the out of plane displacement of the point A (see Figs. 5 and 6).

3.2 Delamination Growth

The use of the fail-release approach in conjunction with the Virtual Crack Closure Technique allows the delamination growth to be taken into account (DEL approach). By adopting this approach is it possible to analyse effects of the delamination propagation on the behaviour of the stiffened panel. The delamination starts growing just after the occurrence of the global buckling causing a modification in the out of plane displacement versus applied strain graph (see Fig. 7): for a fixed applied strain the out of plane displacement obtained in presence of propagation is smaller than the one evaluated without allowing this phenomenon.

Is it possible to find the justification of this sentence is in Fig. 8 where it is visible how the deformed shape of the thin sub-laminate changes as consequence of the delamination opening thus reducing its out of plane displacement. As expected, before the delamination growth nothing changes in terms of structural behaviour. The comparison between the Applied-strain/Load graph obtained by using the CH and DEL approached is not reported here because no relevant differences have been detected between the two curves.

Unfortunately experimental data on the delamination growth initiation load are not available and only delaminated areas at a discrete number of applied loads are provided in Ref. [28].

The numerical and the experimental shape of the delaminated area are compared in Fig. 9: the direction of the propagation and the asymmetry in the opening are very well predicted but the load at which the numerical shape has been obtained is smaller (20%) than the one at which the experimental area is measured.

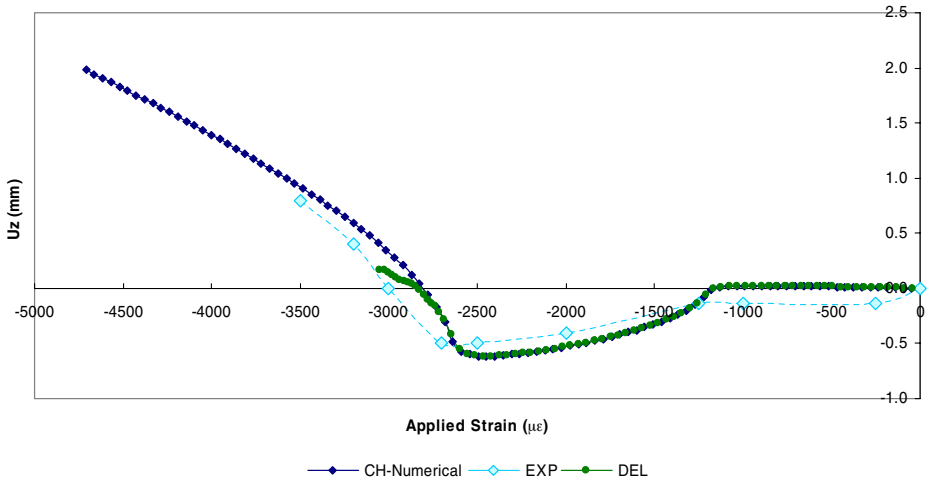

Fig. 7 Applied-strain/Out of plane displacement of the point A: comparison between numerical (CH and DEL approaches) and experimental results

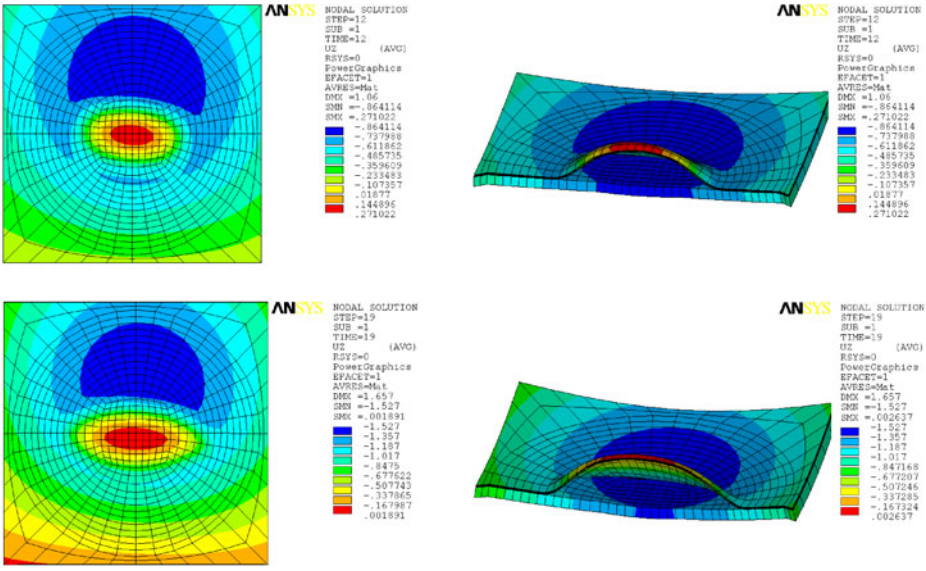

Fig. 8 Deformed shape with out of plane displacement contour for the delaminated area at −2690.58 με (top) [before the delamination starts growing] and −2847.53 με (bottom) [after the beginning of the propagation]

3.3 Intralaminar and Interlaminar Damage Interaction

Finally the behaviour of the stiffened panel has been investigated taking into account also intralaminar damage (matrix/fiber failure)-PDADEL approach. The analysis has been performed up to the −3000 με no significant modifications have been detected between the DEL (Fig. 7) and PDADEL Applied-strain/Load graph curve despite of the onset of matrix and fiber failure in the plies of the thin sub-laminate (see Figs 10, 11 and 12).

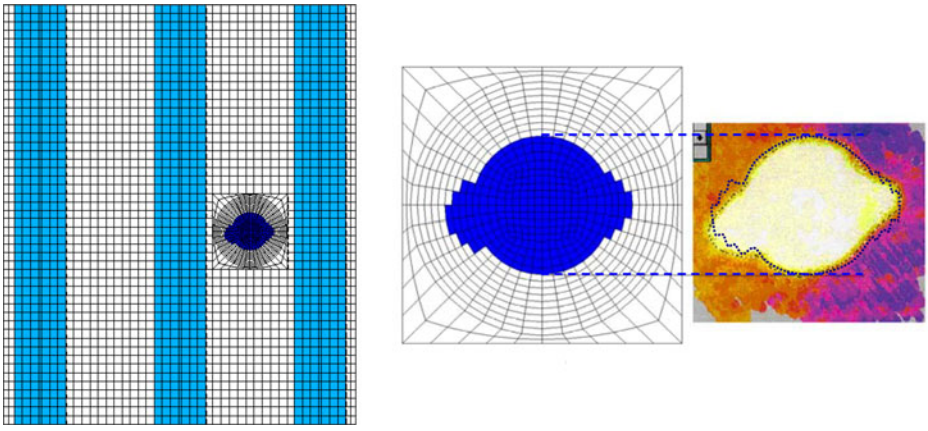

Fig. 9 Comparison between the numerical and the experimental shape of the delaminated area (area obtained at loads whose difference is about 20%)

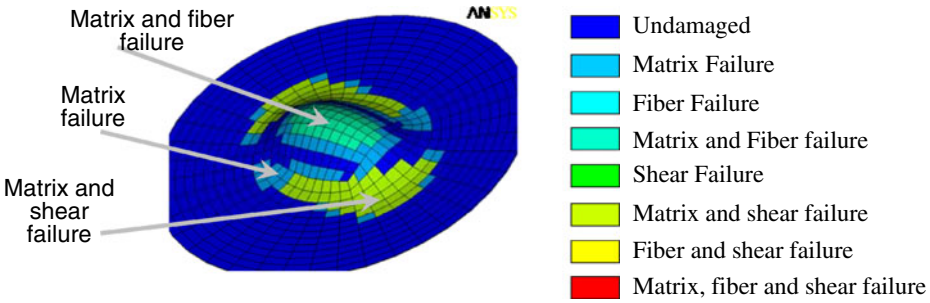

Fig. 10 Intralaminar damage failure. Colours are associated to different damage modes

In fact, at an applied strain equal to −1682 με (FIRST PLY FAILURE), in the most external ply of the thin sub-laminate (+45°) matrix failure and matrix plus shear failure onset where the out of plane displacement is maximum (Fig. 11). As the load increases, the stress redistribution induced by the presence of damage, which in the numerical model is associated to the reduction of the material properties by means of degradation rules (Table 1), leads other elements to fail and the damage zone to extend (Fig. 11 from left to right). The damage progression is shown (Fig. 12) also for the 90° ply of the thin sub-laminate. For this ply the damage onset later respect to the +45° but it grows more rapidly even if only matrix failure is detected.

As said above up to −3000 με the applied-strain/load graph curve does not change respect to the DEL curve however a modification in the Energy Release Rate distribution has been detected (Fig. 13) and induced by the presence of intralaminar damage. Indeed, the direct consequence of this raise in the Energy distribution is an anticipated delamination growth and an increase in the growth rate of the delamination front even if not very pronounced.

4 Discussion and Future Work

The good agreement found between the overall response of the panel (in terms of local and global buckling loads as well as load displacements graph) allows deducing that the global/local approach adopted is very effective indeed. By connecting solid and shell elements it is possible to save computational time in modelling geometrically complex structures; furthermore, finer meshes can be used only where an accurate

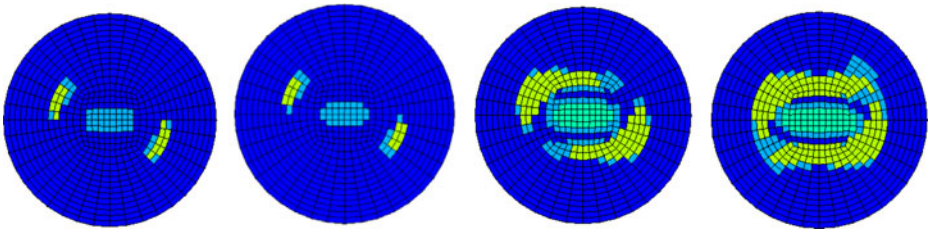

Fig. 11 Failure maps for the −45° ply of the thin sub-laminate: −1682 με (FIRST PLY FAILURE), −1793 με, −2466 με, −2690 με (GROWTH INITIATION)

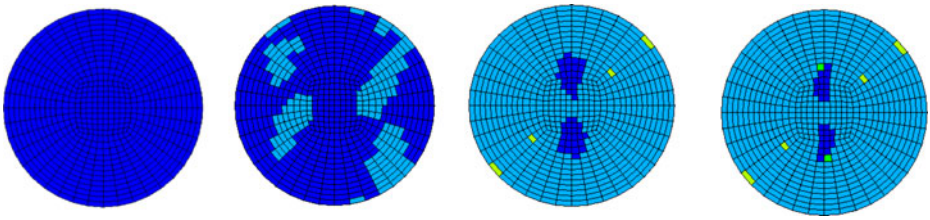

Fig. 12 Failure maps for the +90° ply of the thin sub-laminate: −1682 με, −1793 με, −2466 με, −2690 με

prediction of the three-dimensional state of stress is required (such as zones must prone to be damaged). It is worth noting that the global/local approach employed defines a strong or two-way coupling between the local and the global model therefore effects of one model are passed to the other and vice versa within the same analysis.

Within this paper the intralaminar damage onset has been checked only for elements of the thin sub-laminate lying within a restricted area which is equal to the initial delaminated area plus the surrounding circular crown where the delamination is expected to grow (see Fig. 3- Radius R_{max}). Even if these elements are the most prone to fail, other critical locations could exist within the structure. Thus as further work the extension of the progressive damage approach to the whole structure or to the most critical zones should be foreseen because important also to predict the final failure of the panel.

Further, the propagation of the delamination under stringers and/or the debonding between skin and stringers could be simulated extending opportunely the zones where parts are kept together by releasable connections.

5 Conclusion

The mechanical behaviour of a composite stiffened panel in presence of an embedded delamination within a bay has been analysed. A global/local approach has been adopted to connect differently modeled substructures and its effectiveness has been demonstrated by comparing results with experimental data taken from literature.

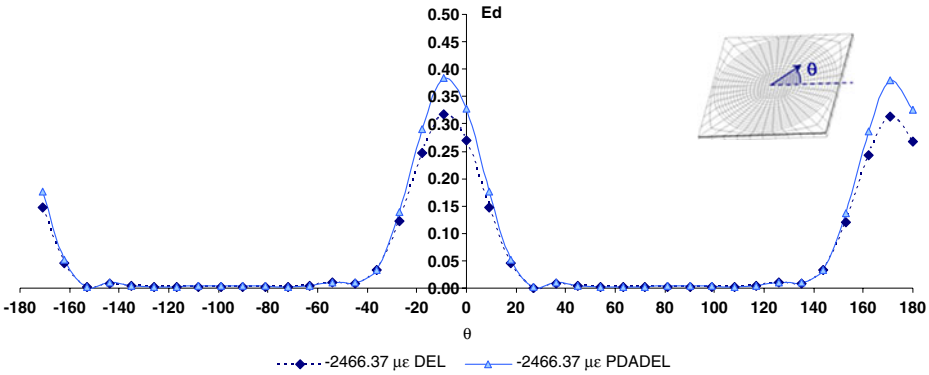

Fig. 13 Energy distribution: comparison between the curve obtained by he approaches DEL and PDADEL (applied deformation −2466.27 με)

Results of three approaches characterized by different levels of detail have been compared in order to highlight effects of each damage type and of their interaction, leading to the observation that intralaminar damage onset and evolution causes an alteration in the Energy distribution at the delamination front inducing a modification in the delamination growth initiation load and in its growth rate.

Acknowledgements The research leading to these results has received funding from the European Community's Seventh Framework Programme FP7/2007–2013 under grant agreement n°213371-MAAX-IMUS. Part of the work reported in this paper has been presented to the 2nd ECCOMAS Thematic Conference on the Mechanical Response of Composites (London, 2009).

References

1. Abrate, S.: Impact on composite structures. Cambridge University Press (1998)
2. Nilsson, K.F., Asp, L.E., Alpman, J.E., Nystedt, L.: Delamination buckling and growth for delaminations at different depths in a slender composite panel. Int. J. Solids Struct. **38**, 3039–3071 (2001)
3. Whitcomb, J.D.: Analysis of a laminate with a postbuckled embedded delamination, including contact effects. Int. J. Compos. Mater. **26**, 1523–1535 (1992)
4. Perugini, P., Riccio, A., Scaramuzzino, F.: Influence of delamination growth and contact phenomena on the compressive behaviour of composite panels. Int. J. Compos. Mater. **33**(15), 1433–1456 (1999)
5. Gaudenzi, P., Perugini, P., Riccio, A.: Post-buckling behaviour of composite panels in the presence of unstable delaminations. Compos Struct **51**, 301–309 (2001)
6. Whitcomb, J.D., Shivakumar, K.N.: Strain-energy release rate analysis of plates with postbuckled delaminations. J. Compos Mater **23**, 714–734 (1989)
7. Whitcomb, J.D.: Instability related delamination growth of embedded and edge delamination, NASA/TM-1988-100655
8. Mukherjee, Y.X., Gulrajani, S.N., Mukherjee, S., Netravali, A.N.: A numerical and experimental study of delaminated layered composites. J. Compos Mater **28**, 837–870 (1994)
9. Nilsson, K.F., Asp, L.E., Sjogren, A.: On transition of delamination growth behaviour for compression loaded composite panels. Int. J. Solids Struct. **38**, 8407–8440 (2001)
10. Sun, X., Tong, L., Chen, H.: Progressive failure analysis of laminated plates with delamination. J. Reinf. Plast. Compos. **20**, 1370–1389 (2001)
11. Liu, S., Chang, F.K.: Matrix cracking effect on delamination growth in composite laminates induced by a spherical indenter. J. Compos. Mater. **28**, 940–977 (1994)
12. Riccio, A., Pietropaoli, E.: Modelling damage propagation in composite plates with embedded delamination under compressive load 2008, 2008, 42(13), 1309–1335.
13. Hellan, K.: Introduction to fracture mechanics. International student edition McGraw Hill Singapore (1985)
14. Krueger, R.: The virtual crack closure technique: history, approach and applications, NASA/CR-2002-211628
15. Reeder, J.R.: An evaluation of mixed-mode delamination failure criteria, NASA-TM-104210
16. Orifici, A.C., de Zarate Alberdi, I.O., Thomson, R.S., Bayandor, J.: Compression and post-buckling damage growth and collapse analysis of flat composite stiffened panels. Compos. Sci. Technol. **68**, 3150–3160 (2008)
17. Hashin, Z.: Failure criteria for unidirectional fibre composites. J. Appl. Mech. **47**, 329–334 (1980)
18. Shokrieh, M., Lessard, L.B.: Progressive fatigue damage modeling of composite materials, Part I: modeling. J. Compos. Mater. **34**, 1056–1115 (2000)
19. Sleight, D.W.: Progressive failure analysis methodology for laminated composite structures, NASA/TP-1999-209107
20. Hahn, H.T., Tsai, S.W.: On the behaviour of composite laminates after initial failures. Astronaut. Aeronaut. **21**, 58–62 (1983)
21. Chanh Fu-Kuo, Chang Huo-Yen: A progressive damage model for laminated composites containing stress concentrations. J. Compos. Mater. **21**, 834–855 (1987)
22. Tan, S.: A Progressive failure model for composite laminates containing openings. J. Compos. Mater. **25**, 556–577 (1991)

23. Engelstad, S.P., Reddy, J.N., Knight, N.F.: Postbuckling response and failure prediction of graphite-epoxy plates loaded in compression. AIAA J. **30**, 2106–2113 (1992)
24. Hahn, H.T., Tsai, S.W.: On the behaviour of composite laminates after initiation failures. J. Compos. Mater. **8**, 288–305 (1974)
25. Chou, S.-C., Orringer, O., Rainey, J.H.: Post-failure behaviour of laminates I-no stress concentration. J. Compos. Mater **10**, 371–381 (1976)
26. Chou, S.-C., Orringer, O., Rainey, J.H.: Post-failure behaviour of laminates II- stress concentration. J. Compos. Mater. **11**, 71–78 (1977)
27. Suemasu, H., Takahashi, H., Ishikawa, T.: On failure mechanisms of composite laminates with an open hole subjected to compressive load. Compos. Sci. Technol. **66**, 634–641 (2006)
28. Greenhalgh, E., Meeks, C., Clarke, A., Thatcher, J.: The effect of defects on the performance of post-buckled CFRP stringer-stiffened panels. Compos. Part A **34**, 623–633 (2003)
29. ANSYS 11.0 user manual
30. Asp, L., Sjogren, A., Greenhalgh, E.: Delamination growth and thresholds in a carbon/epoxy composite under fatigue loading. J. Compos. Technol. Res. **23**, 55–68 (2001)
31. Tsamtsakis, D., Wevers, M., De Meester, P.: Damage monitoring during fatigue loading of quasi-isotropic carbon epoxy laminates, Non destructive testing Van Hemelrijck & Annastassopulos eds, 1996 Balken Rotterdam, ISBN 905410595X